https://doi.org/10.5194/nhess-2020-204
Preprint. Discussion started: 7 August 2020

Natural Hazards and Earth System Sciences
Open Access
Discussions

A revision of the Combined Drought Indicator (CDI) as part of the European Drought Observatory (EDO)

Carmelo Cammalleri[1,*], Carolina Arias-Muñoz[2], Paulo Barbosa[1], Alfred de Jager[1], Diego Magni[3], Dario Masante[3], Marco Mazzeschi[4], Niall McCormick[1], Gustavo Naumann[1], Jonathan Spinoni[1] and Jürgen Vogt[1]

[1] European Commission, Joint Research Centre (JRC), Ispra, Italy.

[2] Arhs Developments, Milan, Italy.

[3] Arcadia SIT, Vigevano, Italy.

[4] UniSystems Luxembourg Sàrl, Luxembourg.

[*] C. Cammalleri (carmelo.cammalleri@ec.europa.eu)

Abstract

Building on almost ten years of expertise and operational application of the Combined Drought Indicator (CDI), which is operationally implemented within the European Commission's European Drought Observatory (EDO) for the purposes of early warning and monitoring of agricultural droughts in Europe, this paper proposes a revised version of the index. The CDI conceptualizes drought as a cascade process, where a precipitation shortage ("WATCH" stage) develops into a soil water deficit ("WARNING" stage), which in turn leads to stress for vegetation ("ALERT" stage). The main goal of the revised CDI proposed here, is to improve the indicator's performance for those events that are currently not reliably represented, without drastically altering the modelling framework. This is achieved by means of two main modifications: (a) use of the previously

https://doi.org/10.5194/nhess-2020-204
Preprint. Discussion started: 7 August 2020

occurring CDI value to improve the temporal consistency of the timeseries, (b) introduction of two temporary classes - namely, soil moisture and vegetation greenness - to avoid brief discontinuities in a stage. The efficacy of the modifications is tested by comparing the performances of the revised and currently implemented versions of the indicator, for actual drought events in Europe during the last 20 years. The revised CDI reliably reproduces the evolution of major droughts, out-performing the current version of the indicator, especially for long-lasting events. Since the revised CDI does not need supplementary input datasets, it is suitable for operational implementation within the EDO drought monitoring system.

Keywords: agricultural drought, SPI, soil moisture, FAPAR, drought monitoring.

1. Introduction

In the past 20 years, the monitoring of drought events has gained increasing relevance thanks to the shift in the paradigm for drought risk management from a reactive to a proactive approach (Wilhite and Pulwarty, 2005). As advocated by WMO and GWP (2014), drought monitoring and early warning systems represent one of the three main pillars for successful integrated drought management (the others being vulnerability and impact assessment, and drought preparedness, mitigation, and response). A drought monitoring and early warning system identifies climate and water resources trends and detects the emergence or probability of occurrence and the likely severity of droughts and its impacts, and should provide reliable information about impending drought conditions that can be timely communicated to water managers, policy makers, and the public (Vogt et al., 2018a).

As one of the six core services of the European Union's Copernicus Earth observation programme, the Copernicus Emergency Management Service (https://emergency.copernicus.eu/)

https://doi.org/10.5194/nhess-2020-204
Preprint. Discussion started: 7 August 2020

includes two closely related systems for drought monitoring and early warning at the European and global levels, namely the European Drought Observatory (EDO; https://edo.jrc.ec.europa.eu/) and the Global Drought Observatory (GDO; https://edo.jrc.ec.europa.eu/gdo/). At the European scale, EDO provides a comprehensive set of tools for monitoring and early detection of drought conditions, with indicators aimed at both expert users and policy-makers (Vogt et al., 2018b).

Among the high-level synthetic descriptors of droughts that are implemented in EDO, the Combined Drought Indicator (CDI) provides a concise representation of the evolution of agricultural droughts, suitable for communication to both specialized end-users and the general public. The CDI, originally conceived by Sepulcre-Canto et al. (2012), has been successfully applied within EDO as part of a near-real time monitoring with dekadal (roughly 10 days, 3 times at month) updates and a time-lag of just a few days.

Throughout almost 10 years of its operational use in EDO, the CDI has proved itself effective at reliably capturing the start and development of most of the severe droughts that affected European countries during this time, as documented by the analytical drought reports that are regularly published through the EDO web portal (https://edo.jrc.ec.europa.eu/edov2/php/index.php?id=1051). Maps of EDO's CDI have also been extensively used by the European Commission's Emergency Response Coordination Centre (ERCC), for their daily maps on the most important ongoing emergency events (https://erccportal.jrc.ec.europa.eu/Maps/Daily-maps).

While the CDI can claim a considerable number of successful applications in the cases of recognized drought events, a day-by-day analysis of its various components has led to an increased understanding of its behaviour, and has also highlighted potential improvements, particularly with regard to its temporal consistency in the case of long-lasting events. The resulting expertise, which is based on extensive practical experience and a long history of actual cases, can

https://doi.org/10.5194/nhess-2020-204
Preprint. Discussion started: 7 August 2020

be used to improve the indicator's performance in those circumstances where it currently may fall short of expectations. However, any changes to the modelling framework of an established indicator such as the CDI, must take into account the existing considerable community of users, who are accustomed to the indicator in its current form. In addition, its acceptance within the scientific community as a recognized indicator (e.g. Clark et al., 2016; Mariani et al., 2018; WMO and GWP, 2016), which is further exemplified by its use in major case-studies and inter-comparison analyses (e.g. Blauhut et al., 2016; Jiménez-Donaire et al., 2020; Schwarz et al., 2020), must also be carefully considered prior to making any modifications.

In light of these considerations, the main goal of this paper is to propose a revised version of the CDI, with a focus on improving the overall quality of the indicator's performance without substantially altering the original concept, or undermining the results achieved over many documented successful case studies. The performance of the revised version of the indicator is evaluated against the main drought events in Europe during the past 20 years, and by means of a direct inter-comparison with the current version of the indicator that is operational implemented within EDO.

2. Material and Methods

In this section, the input datasets that are used for computing the CDI are described, and the computation methods that are applied in both the current version and proposed revision of the indicator are outlined. Two sets of case studies of past drought events, covering the years 2001-2018 - which are used to compare the performances of the current and proposed new versions of the indicator - are also summarised.

2.1 Input datasets

The Combined Drought Indicator (CDI) is computed on the basis of the inter-dependency of three

https://doi.org/10.5194/nhess-2020-204
Preprint. Discussion started: 7 August 2020

main variables: precipitation, soil moisture, and vegetation greenness. The values for each of these quantities are standardized as deviations from historical climatology, and compared with a threshold value to discriminate between normal and extreme conditions. While the data processing approach is conceptually analogous for all three variables, some peculiarities (for example regarding the data's spatiotemporal resolution, and reference baseline) are worth highlighting, and these are described in the following sub-sections.

2.1.1 Precipitation

Monthly precipitation maps at a spatial resolution of 0.25 degrees are derived by blending daily rainfall observations at SYNOP (Surface Synoptic Observations) stations from the MARS database (http://mars.jrc.ec.europa.eu/) of the European Commission's Joint Research Centre (JRC), with monthly precipitation maps at a spatial resolution of 1.0 degree from the Global Precipitation Climatology Centre (GPCC, http://gpcp.dwd.de).

The 1-month and 3-month Standardized Precipitation Index (SPI-1 and SPI-3, respectively) are calculated using the two-parameter gamma distribution fitted over a 30-year reference period (1981-2010) using the maximum likelihood estimators of Thom (1958) and Greenwood and Durand (1960). SPI-3 is selected because of its documented correlation with agricultural drought (WMO, 2012), whereas SPI-1 is selected due to its suitability for detecting the possible occurrence of "flash droughts" (when combined with increased evaporative demand due to high temperatures, low humidity and/or strong winds), as described by Otkin et al. (2018). In line with Sepulcre-Canto et al. (2012), a threshold value of -1.0 is used for SPI-3, marking the start of moderately dry conditions according to McKee et al. (1993), whereas a threshold value of -2.0 is used for SPI-1, denoting the start of extremely dry conditions.

For computing the CDI, both SPI indicators are used jointly to detect precipitation shortages. Hence, for the sake of simplicity a Boolean SPI indicator (zSPI) is defined, which assumes a value of

https://doi.org/10.5194/nhess-2020-204
Preprint. Discussion started: 7 August 2020

Natural Hazards and Earth System Sciences
Open Access
EGU
Discussions

1 if either SPI-1 or SPI-3 reports a dry status, as follows:

$$\text{zSPI} = \begin{cases} 1 & \text{SPI-3} < -1 \quad \textit{or} \quad \text{SPI-1} < -2 \\ 0 & \textit{otherwise} \end{cases} \tag{1}$$

2.1.2 Soil Moisture

The soil moisture anomaly index (zSM) is computed using the modelled soil moisture output of the LISFLOOD hydrological precipitation-runoff model (De Roo et al., 2000). Firstly, dekadal (roughly 10-day) maps of the Soil Moisture Index (SMI; Seneviratne et al., 2010) are computed at a spatial resolution of 5 km, as a weighted average of the daily volumetric soil moisture values produced by LISFLOOD for the skin and root zone layers. Successively, the zSM is computed as standardized deviations (i.e. z-scores) of the values from the full available period (1995-2018).

In the present study, SMI replaces the soil suction (pF) that was previously used both within EDO and for the original development of the CDI. This has been done as part of a reorganization of the EDO data portal, in order to improve the readability of maps for non-expert users, given that SMI simply ranges from 0 (dry) to 1 (wet). Since both SMI and pF are derived from the same daily volumetric soil moisture dataset and using the same pedotransfer function (PTF; Laguardia and Niemeyer, 2008), the obtained zSM maps are in practical terms the opposite to the "Anomaly pF" used in Sepulcre-Canto et al. (2012). Following these considerations, a threshold of -1 is adopted to discriminate dry conditions in zSM, analogously to what is used for SPI-3.

2.1.3 Vegetation greenness

In this study, the biophysical variable Fraction of Absorbed Photosynthetically Active Radiation (FAPAR), which is estimated from satellite remote sensing data, is used as a proxy for the health status of vegetation. Sepulcre-Canto et al. (2012) adopted the 10-day composite FAPAR images provided by ESA, derived from the Medium Resolution Imaging Spectrometer (MERIS) on board of

https://doi.org/10.5194/nhess-2020-204
Preprint. Discussion started: 7 August 2020

the ENVISAT platform. Following the failure of ENVISAT in 2012, the MOD15A2H Collection 6 FAPAR product (Myneni, 2015), as derived from the Moderate-Resolution Imaging Spectroradiometer (MODIS) sensor on board of the Terra satellite, has been used as replacement in the operational implementation of the CDI.

The MOD15A2H product is provided by NASA at spatial resolution of 500 metres, as 8-day maximum composites. Within EDO, these raw data are re-projected onto a 0.01 degrees latitude/longitude regular grid, and dekadal maps are derived by means of a weighted average of the two closest 8-day maps followed by an exponential smoothing (Cammalleri et al., 2019). As in the case for soil moisture, anomalies of FAPAR (zFAPAR) are computed as a standardized z-score on the full available dataset baseline period (2001-2018). Also in this case, a threshold value of -1.0 is adopted to highlight dry conditions.

2.2 The current version of CDI, as implemented in EDO (CDI-v1)

As is described in detail by Sepulcre-Canto et al. (2012), in the modelling framework of the CDI the evolution of a drought event is conceptualized by a "cause-effect" relationship, assuming that a shortage in precipitation leads to a soil moisture deficit, culminating in reduced vegetation productivity. In its original form, data for the variables zSPI, zSM and zFAPAR (see above) are used to characterize three stages of an idealized agricultural drought:

- "WATCH", in which the precipitation is below normal (zSPI = 1), and an early warning signal of a potential drought affecting agriculture can be observed;
- "WARNING", when a precipitation deficit propagates in the hydrological cycle and affects soil water content (zSPI = 1 & zSM < -1).
- "ALERT", when the effects of drought become visible as vegetation stress (zSPI = 1 & zFAPAR < -1).

https://doi.org/10.5194/nhess-2020-204
Preprint. Discussion started: 7 August 2020

During the operational implementation of the indicator, two additional recovery stages were introduced (see https://edo.jrc.ec.europa.eu/documents/factsheets/), aimed at better capturing the "fade-out" phase of a drought, namely the "PARTIAL RECOVERY" and "FULL RECOVERY" stages. In both stages, the previous month's zSPI ($zSPI_{m-1}$) is introduced to account for the preceding conditions:

- "PARTIAL RECOVERY": zSPI returns to normal values even if vegetation is still negatively affected ($zSPI_{m-1} = 1$ & $zSPI = 0$ & $zFAPAR < -1$).
- "FULL RECOVERY": Both precipitation and FAPAR return to normal conditions ($zSPI_{m-1} = 1$ & $zSPI = 0$ & $zFAPAR \geq -1$).

This operational implementation of the index is the one commonly referred to in the scientific and technical drought literature when CDI is described.

The CDI modelling framework described above is summarised in Fig. 1, where the different stages of CDI (from WATCH to FULL RECOVERY) are depicted according to the eight cases that can be obtained by combining the two possible binary states for each of the three main variables (zSPI, zSM, zFAPAR), as well as a function of $zSPI_{m-1}$.

Due to its operational status, the maps of the CDI that are currently available in EDO are always processed using data available up to the release date of a new map. For this reason, some inconsistencies in the reference baseline and actual data (e.g. FAPAR data source) are present in this operational dataset. For the present study, a self-consistent dataset has been produced by re-computing the CDI with the best data available at the end of 2018. This dataset (referred to here as CDI-v1) is consists of 648 dekadal maps at 5-km spatial resolution, from January 2001 to December 2018. In order to compute the CDI at this spatial resolution, the original data for zSPI and zFAPAR were initially resampled over the zSM grid, using the nearest neighbour and spatial average procedure, respectively.

https://doi.org/10.5194/nhess-2020-204
Preprint. Discussion started: 7 August 2020

2.3 The revised version of CDI, as proposed here (CDI-v2)

In order to better understand the modifications to the CDI that are proposed here, two case studies where CDI-v1 was not able to capture in full the evolution of the drought, are first reported.

The original concept behind the CDI assumes the sequential occurrence of extreme conditions detected by the three constituent indicators (SPI, soil moisture anomalies, and FAPAR anomalies). In fact, while Sepulcre-Canto et al. (2012) illustrated the CDI scheme as a cascade process (see the schematisation in that paper Fig. 1), its actual implementation can be seen more in the context of a nested approach, since each successive stage is contained within the definition of the previous one. This is exemplified by the inclusive nature of the calculation (see above, where "&" is used in the definition of the classes). This approach can lead to abrupt breaks in tracking a drought event, when a substantial temporal shift among the three quantities can be observed.

For example, the plots in Fig. 2 report the timeseries of SPI-3 (upper panel), zSM (middle panel) and zFAPAR (lower panel) for a year that includes a drought event in Spain. Dotted vertical lines demarcate the full span of the drought event. At the top of each plot, a box demarcates the period when the stage-specific conditions for WATCH, WARNING and ALERT are met. By an *a posteriori* analysis of the event, it is easy to assess a desirable sequence of stages for each dekad, as reported in the bottom part of the lower plot (i.e. the ideal outcome of a revised CDI, CDI-v2 ideally). However, from the actual sequence of CDI values (CDI-v1) it can be seen that the event is interrupted in the middle of the soil moisture deficit period due to the return of precipitation to normal conditions.

A second example is shown in Fig. 3 for a drought event in France, where the timeseries of SPI-3, zSM and zFAPAR suggests an extensive period of soil moisture deficit following a

https://doi.org/10.5194/nhess-2020-204
Preprint. Discussion started: 7 August 2020

precipitation deficit, that caused a short period of FAPAR anomalies. Even if two periods meeting the requirement for a WARNING and an ALERT status are observed (see boxes at the top of the middle and lower panels, respectively), a temporary return above the thresholds is observed (for one or two dekads) in both zSM and zFAPAR timeseries. In an *a posteriori* analysis, a single continuous ALERT period would have been likely detected (see ideal CDI sequence at the bottom of the Figure). CDI-v1 instead treats those gaps as interruptions, causing a "back-and-forth" transition between the ALERT and WARNING stages.

This behaviour is in contrast to the "cause-effect" principle on which the indicator is based, and even if this occurrence cannot be always avoided in real case studies, it should be kept to a minimum. It is worth noting how, also in this second case, according to CDI-v1 the event stops well before the end of the soil moisture deficit, due to the return of precipitation to normal conditions (SPI-3 > -1).

The two examples reported above highlight the main drawbacks of the current operational version of the CDI, which can be summarized as follow:

- Lack of a proper cascade process in favour of a nested approach, which can cause an early interruption in drought events in case of notable shifts between timeseries;
- absence of check on the possible small gaps within a stage, which can lead to inconsistencies in the temporal sequence and quick alternation of different stages.

The revised version of the CDI that is proposed here (i.e. CDI-v2 from hereafter) addresses these two key issues by introducing two principal modifications:

- Set-up different rules to ensure temporal continuity based on the previous dekad's CDI (CDI_{d-1}) rather than the preceding SPI (SPI_{m-1});
- adding a second set of threshold values to detect both temporary gaps within a stage, and

https://doi.org/10.5194/nhess-2020-204
Preprint. Discussion started: 7 August 2020

the "fade-out" phase of a drought.

These modifications are implemented according to the scheme depicted in Fig. 4, where the upper part of the Table is analogous to that of Fig. 1, whereas the lower part details the values assumed by the index for all the possible cases of preceding CDI values.

By juxtaposing Figs. 1 and 4, it is possible to highlight the main changes introduced after discriminating the outputs on the basis of CDI_{d-1}. On the one hand, it is possible to notice how CDI-v2 (i.e. the proposed revision) behaves identically to CDI-v1 (i.e. the current version) at the start of a new event (first row, CDI_{d-1} = 0 or 4). On the other hand, for an on-going event (CDI_{d-1} = 1,2,5,3,6), CDI-v2 still behaves similarly to CDI-v1 for the combinations *a-b* and *f-h*, whereas some major differences can be observed for the cases *c-e*. In these latter instances, both the WARNING and ALERT stages are preserved if zSM and zFAPAR values support these conditions independently from the value of zSPI. This modification aims at solving the problem highlighted by the example in Fig. 2.

The lower part of the table in Fig. 4 highlights how the inclusion of a second threshold for zSM and zFAPAR (i.e. 0.0 in both cases) aims at addressing those situations when the CDI tends to return to a stage that conceptually precedes that of the previous dekad (i.e. a WARNING following an ALERT). In all these circumstances, two TEMPORARY RECOVERY stages are introduced - one for soil moisture and one for FAPAR - if the values of zSM or zFAPAR fall in between the two threshold values (i.e. -1.0 and 0.0). Since these classes are meant to be temporary, we wanted to avoid that the index remains locked in these classes for long periods of time. For this reason, a constrain on the maximum duration of the TEMPORARY RECOVERY stages is fixed at 4 dekads. This value is chosen as the minim length to ensure the inclusion of two consecutive monthly zSPI values.

2.4 Case studies during past drought events

The performance of the current version and proposed revision of the CDI (called CDI-v1 and CDI-v2 in this paper, respectively) is evaluated over two datasets of past drought events in Europe occurred during the period 2001-2018 (years when all the input datasets are overlapping). The first dataset comprises the drought events that were used by Sepulcre-Canto et al. (2012) to test the original implementation of the CDI. These include: the major 2003 drought in central Europe, using data from Madegburg (DE), Ciampino (IT) and Wattisham (UK); the 2004-2005 drought affecting the Iberian Peninsula, using data from Albacete (ES) and Beja (PT); the 2007 drought in Italy, using data from Ciampino (IT); and the 2011 drought affecting western Germany and France, using data from Madegburg (DE) and Deols (FR).

The second dataset of past drought events that was used to assess the performance of both versions of the CDI, is derived from the major droughts that have been documented in EDO (https://edo.jrc.ec.europa.eu/edov2/php/index.php?id=1051) since the CDI has been operationally implemented. These include: the 2012 drought affecting western Europe, using data from Lisbon (PT); the 2014 drought in eastern Spain, using data from Valencia (ES); the 2015 drought in central Europe, using data from Strasbourg (FR); the summer 2017 drought in central Italy, using data from Rome (IT); and the major 2018 drought in northern Europe, using data from Dublin (IE), Hannover (DE), Poznan (PL) and Silkeborg (DK).

3. Results and Discussion

Following the modification introduced, one of the main improvements that may be expected in the revised version of the CDI (CDI-v2) is concerning temporal consistency at the local scale. For this reason, an initial test was made to compare the temporal behaviour of the current version (CDI-v1) and proposed revision (CDI-v2) of the indicator, over selected locations in Europe, during well-documented drought events.

The plots in Figs. 5 and 6 show dekadal timeseries of CDI-v1 (upper line) and CDI-v2 (lower

https://doi.org/10.5194/nhess-2020-204
Preprint. Discussion started: 7 August 2020

line), with the colours corresponding to the classifications in Figs. 1 and 4, respectively. The sites in Fig. 5 correspond to the locations used for validation by Sepulcre-Canto et al. (2012), whereas the sites in Fig. 6 were extrapolated from the detailed reports of EDO for the most recent drought events.

In all the cases studied, the start of the drought event coincides for the two versions of the indicator (CDI-v1 and CDI-v2), as is to be expected given the analogous conditions adopted to define a new event. Over some sites, the two versions do not differ substantially, as in the case of Wattisham and Magdeburg (Fig. 5), and Silkeborg and Poznan (Fig. 6), where only minor signs of the issues highlighted in Figs. 2 and 3 can be observed. In those study sites, the temporal evolution of the droughts appears to be well reproduced by both versions of the indicator, with the start-, peak- and end-dates consistent with the scientific literature for the events (Buras et al., 2020; Ciais et al., 2005; Hanel et al., 2018; Rebetez et al., 2006).

Conversely, the drought development for the sites of Albacete (2005 drought), Ciampino (2007 drought), Lisbon (2012 drought) and Valencia (2014 drought), differs substantially for the revised version (CDI-v2) compared to the current version (CDI-v1), with an overall longer duration and prolonged periods under the WARNING and ALERT stages. The drought events at those sites are rather similar to that depicted in Fig. 2, with a long period of soil water deficit and plant water stress during the whole dry season following a rainfall deficit early in spring and a hot and dry summers. In these cases, the new version of the index seems capable to capture those instances when a drought is prolonged by higher than normal evaporative demand even after the rainfall returns to normal. Considering the well documented severity of those droughts (Garcia-Herrera et al., 2007; MeteoAM, 2007; Spinoni et al., 2015), the behaviour of CDI-v2 seems much more in line with the expected evolution of the droughts.

Finally, for some study cases - specifically Deols (2011 drought), Strasbourg (2015 drought) and Dublin (2018 drought) - the erratic behaviour of CDI-v1 that is evident later in the event (similar to the example of Fig. 3), is replaced by a noticeably smoother dynamic in CDI-v2, which is more in line with both the desirable sequencing of stages and the expected behaviour of a slow-evolving phenomenon such as drought.

For most of the test sites, the representation of the temporal evolution of the drought events by CDI-v2 better fits the conceptual “cause-effect” framework of the indicator, by reducing inconsistent changes in the drought stages. This is quantified by the data reported in Table 1, where the percentage of cells experiencing a stage sequencing in contrast with the “cause-effect” modelling (i.e. a dekad with WARNING followed by one with WATCH) are reported. These data, expressed as average percentage of the area affected by drought (i.e. the sum of all stages excluding FULL RECOVERY), show a drastic decrease when the CDI-v2 is used instead of CDI-v1. The reduction occurs in all the three cases considered, with an overall percentage that goes from about 7% for CDI-v1 to just 2% for CDI-v2. This result, in combination with the aforementioned matching in the start of the drought events between the two versions, show a better capability of the revised indicator (CDI-v2) to capture the evolution of the droughts compared to the current version (CDI-v1).

By expanding the analysis to the full spatial extent of the drought events, some considerations on the spatial patterns of the current (CDI-v1) and revised (CDI-v2) versions of the indicator can be extrapolated. Some key features are summarised in Figs. 7 to 10 for the major droughts in central Europe (2003), the Iberian Peninsula (2005), central Europe (2011), and northern Europe (2018). In each case, the upper plot shows the percentage of the area affected by drought (i.e. the sum of all stages excluding FULL RECOVERY) for each month, whereas the maps show examples of the CDI’s spatial distribution for selected dekads during the event (as demarcated by squares on the upper-plot’s X-axis).

In all four study cases, it is evident how the percentage of the area that is considered under drought has a similar temporal behaviour for the two current and revised versions of the indicator, with the latter having only a slightly larger spatial coverage later in the events. An examination of the maps, however, shows that even if the total area affected is similar, the partitioning among the different stages may drastically differ around the peak of the drought. Indeed, the maps for CDI-v1 and CDI-v2 look quite similar at the beginning of the events, but in the case of CDI-v2 these become much more uniform, and with a higher number of cells under the ALERT stage, later in the event. Considering the temporal correspondence of these maps, the stage depicted by CDI-v2 seems to be much more in line with the expected outcomes at the peak of the most severe European droughts.

In some circumstances (e.g. Fig. 8, between July and August), the current version (CDI-v1) depicts rather different patterns for two consecutive dekads, whereas the revised version (CDI-v2) gives outcomes that are more temporally consistent, especially when comparing successive maps. Overall, the spatial patterns for the different stages appear to be more uniform for CDI-v2 compared with CDI-v1, even if both indicators are computed separately for each cell without any specific constraint on spatial consistency.

Finally, in order to analyze further the evolution of the partitioning of drought stages during a drought event, the plots in Fig. 11 show the timeseries of the percentage differences between CDI-v1 and CDI-v2, in the fraction of the area in the WATCH, WARNING and ALERT stages, for the same four main droughts that are depicted in Figs. 7-10. Those plots show no substantial differences at the beginning of each event (first 2/3 months), and a reduction in the WATCH fraction for CDI-v2 (negative differences) in favour of an increase in the WARNING and ALERT fractions (i.e. the first and later stages), during the development of the events. The results are consistent across the different events, suggesting that the behaviour of the revised version of the indicator (CDI-v2) better reflects the “cause-effect” principle by showing a progressive representation of the drought. For example, in Fig. 11, some areas that are classified as WATCH by CDI-v1, are marked as WARNING and ALERT by CDI-v2, with an increased percentage of WARNING preceding the peak of the drought (June-July in 2003; April in 2011; and May-June in 2018), and an increased percentage of ALERT at the peak of the event (September in 2003 and 2018; July in 2011; and August-September in 2005).

4. Summary and Conclusions

A revised version of the Combined Drought Indicator (CDI), which is currently implemented operationally within the European Commission’s European Drought Observatory (EDO) for providing early warning and monitoring of agricultural droughts, has been analysed. The proposed revision of the CDI is based on the extensive experience that has been gained from applying the indicator during several major drought events that have affected different parts of Europe over the last ten years.

While the current version of the CDI (called CDI-v1 in this paper) has successfully captured the onset of most of the documented major drought events, its ability to track correctly evolution of events has been limited in the case of long lasting droughts with significant temporal shift between reduced rainfall, soil moisture deficit and vegetation stress periods caused by high temperature and evaporative demand following the rainfall deficit. The proposed revision of the CDI (called CDI-v2 in this paper) aims at addressing those shortcomings, without substantially altering the conceptual “cause-effect” framework underlying its original development, especially given the indicator’s proven reliability based on many case-studies and inter-comparison analyses. In general, both the input dataset requirements and the threshold values used to identify extremes conditions, remain unaltered in the revised version of the indicator. This enables the

https://doi.org/10.5194/nhess-2020-204
Preprint. Discussion started: 7 August 2020

retroactive application of the revised indicator to past drought events, without the need for additional inputs or changes in the underlying datasets. For similar reasons, the three main stages of drought (i.e. "WATCH", "WARNING" and "ALERT"), which were originally defined in Sepulcre-Canto et al. (2012), remain unchanged, as does the inclusion of a "FULL RECOVERY" stage to identify the end of a drought period and the return to normal conditions.

The two main changes that are introduced in the CDI-v2 are:

- The inclusion of a constraint on the temporal consistency, based on the CDI's value in the preceding dekad (thus rendering obsolete the previously defined "PARTIAL RECOVERY" stage).
- The addition of two "TEMPORARY RECOVERY" stages - one for soil moisture and the other for FAPAR (representing vegetation greenness) – with the aim of improving the temporal continuity, in the case of small gaps in the middle of periods that are otherwise characterised by the same drought stage.

A comparison of the performance of the current version (CDI-v1) and proposed revision (CDI-v2) of the indicator highlights CDI-v2's capability to improve on the results of CDI-v1 in several circumstances, without negatively affecting the overall performance for drought events that are already correctly reproduced by CDI-v1. This is suggested by the reduced number of instances when a certain stage is followed by another that is not coherent with the "cause-effect" modelling framework.

While for a few test cases (e.g. the 2018 drought in northern Europe), only marginal changes are observed, in the majority of the cases the new version of the indicator (CDI-v2) clearly outperforms the current version, with an overall better temporal consistency and a more continuous sequencing of the drought stages. In all the observed study cases, the CDI-v2 returns a reduced number of cells under WATCH around the peak of the drought in favour of WARNING (before the peak) and ALERT (at the peak) stages.

https://doi.org/10.5194/nhess-2020-204
Preprint. Discussion started: 7 August 2020

On a general level, it is apparent that both the point-scale timeseries and the spatial maps obtained with the new version of the indicator, better approximate the expected spatiotemporal characteristics of a drought event, with a more realistic succession of the “WATCH”, “WARNING” and “ALERT stages”, and a large spatial consistency in the modelled patterns. In addition, in spite of the improved performance of the revised version of the CDI, the “look and feel” of the indicator are not substantially altered. Given the well established and wide community of users of the current version of the CDI that is implemented in EDO, this is a key consideration that can ensure a smooth transition to the operational use within EDO, of the revised version of the CDI that is proposed here.

https://doi.org/10.5194/nhess-2020-204
Preprint. Discussion started: 7 August 2020

References

Blauhut, V., Stahl, K., Stagge, J.H., Tallaksen, L.M., De Stefano, L. and Vogt, J.: Estimating drought risk across Europe from reported drought impacts, drought indices, and vulnerability factors, Hydrol. Earth Syst. Sci., 20, 2779-2800, doi:10.5194/hess-20-2779-2016, 2016.

Buras, A., Rammig, A. and Zang, C.S.: Quantifying impacts of the drought 2018 on European ecosystems in comparison to 2003, Biogeosciences, 17, 1655-1672, doi:10.5194/bg-17-1655-2020, 2020.

Cammalleri, C., Verger, A., Lacaze, R. and Vogt, J.V.: Harmonization of GEOV2 FAPAR time series through MODIS data for global drought monitoring, Int. J. Appl. Earth Obs. Geoinf., 80, 1-12, doi:10.1016/j.jag.2019.03.017, 2019.

Ciais, P., Reichstein, M., Viovy, N., Granier, A., Ogée, J., Allard, V., Aubinet, M., Buchmann, N., Bernhofer, C., Carrara, A., Chevallier, F., De Noblet, N., Friend, A.D., Friedlingstein, P., Grünwald, T., Heinesch, B., Keronen, P., Knohl, A., Krinner, G., Loustau, D., Manca, G., Matteucci, G., Miglietta, F., Ourcival, J.M., Papale, D., Pilegaard, K., Rambal, S., Seufeet, G., Soussana, J.F., Sanz, M.J., Schulze, E.D., Vesala, T. and Valentini, R.: Europe-wide reduction in primary productivity caused by the heat and drought in 2003, Nature, 437, 529-533, doi:10.1038/nature03972, 2005.

Clark, A., McGowen, I., Crean, J., Kelly, R. and Wang, B.: Stage 1 – Enhanced Drought Information System: NSW DPI Combined Drought Indicator. Technical Report, NSW Department of Primary Industries, ISBN 978-1-76058-016-2, 76 pp, 2016.

De Roo, A., Wesseling, C. and Van Deursen, W.: Physically based river basin modeling within a GIS: The LISFLOOD model, Hydrol. Process., 14, 1981-1992, doi:10.1002/1099-1085(20000815/30)14:11/12<1981::AID-HYP49>3.0.CO;2-F, 2000.

Garcia-Herrera, R., Paredes, D., Trigo, R.M., Trigo, I.F., Hernandez, H., Barriopedro, D. and Mendes, M.T.: The outstanding 2004-2005 drought in the Iberian Peninsula: associated atmospheric circulation, J. Hydrometeorol., 8, 483–498, doi:10.1175/JHM578.1, 2007.

Greenwood, J.A. and Durand, D.: Aids for fitting the gamma distribution by maximum likelihood, Technometrics, 2, 55-65, doi:10.1080/00401706.1960.10489880, 1960.

Hanel, M., Rakovec, O., Markonis, Y., Máca, P., Samaniego, L., Kyselý, J. and Kumar, R.: Revisiting the recent European droughts from a long-term perspective, Sci. Rep., 8, 9499, doi:10.1038/s41598-018-27464-4, 2018.

Laguardia, G. and Niemeyer, S.: On the comparison between the LISFLOOD modeled and the ERS/ASCAT derived soil moisture estimates, Hydrol. Earth Syst. Sci., 12, 1339-1351, doi:10.5194/hess-12-1339-2008, 2008.

Jiménez-Donaire, M., Tarquis, A. and Giráldez, J.V.: Evaluation of a combined drought indicator and its potential for agricultural drought prediction in southern Spain, Nat. Hazards Earth Syst. Sci., 20, 21-33, doi:10.5194/nhess-20-21-2020, 2020.

Mariani, S., Braca, G., Romano, E., Lastoria, B. and Bussettini, M.: Linee Guida sugli Indicatori di Siccità e Scarsità Idrica da utilizzare nelle attività degli Osservatori Permanenti per gli Utilizzi Idrici - Stato Attuale e Prospettive Future (in Italian), Technical Report, CREiAMO PA, 56 pp., 2018.

McKee, T.B., Doesken, N.J. and Kleist, J.: The relationship of drought frequency and duration to time scales, in: Proceedings of the 8th Conference of Applied Climatology, Anaheim, CA, Am. Meteorol. Soc. 179-184, 1993.

MeteoAM, 2007. Climatologia – temperatura e precipitazioni Aprile 2007, available at: http://clima.meteoam.it/bollettinoMensile.php, last access: 10 March 2020.

Myneni, R.B.: MOD15A2H MODIS/Terra leaf area Index/FPAR 8-Day L4 global 500m SIN grid V006. NASA EOSDIS Land Processes DAAC, doi:10.5067/modis/mod15a2h.006, 2015.

Otkin, J.A., Svoboda, M., Hunt, E.D., Ford, T.W., Anderson, M.C., Hain, C. and Basara, J.B.: Flash

https://doi.org/10.5194/nhess-2020-204
Preprint. Discussion started: 7 August 2020

droughts: A review and assessment of the challenges imposed by rapid-onset droughts in the United States, Bull. Amer. Meteor. Soc., 99, 911-919, doi:10.1175/BAMS-D-17-0149.1, 2018.

Pischke, F. and Stefanski, R.: Integrated Drought Management Initiatives, in: Wilhite D.A. and Pulwarty R.S. (Eds.). Drought and Water Crises: Integrating Science, Management and Policy (Chapter 3), CRC Press (Taylor & Francis), Boca Raton, 39-54, 2018.

Rebetez, M., Mayer, H., Dupont, O., Schindler, D., Gartner, K., Kropp, J.P. and Menzel, A.: Heat and drought 2003 in Europe: A climate synthesis, Ann. For. Sci., 63, 569-577, doi:10.1051/forest:2006043, 2006.

Schwarz, M., Landmann, T., Cornish, N., Wetzel, K.-F., Siebert, S. and Franke, J.: A spatially transferable drought hazard and drought risk modeling approach based on remote sensing data, Remote Sens., 12(2), 237, doi:10.3390/rs12020237, 2020.

Sepulcre-Canto, G., Horion, S., Singleton, A., Carrao, H. and Vogt, J.: Development of a Combined Drought Indicator to detect agricultural drought in Europe, Nat. Hazards Earth Syst. Sci., 12, 3519-3531, doi:10.5194/nhess-12-3519-2012, 2012.

Spinoni, J., Naumann, G., Vogt, J.V. and Barbosa, P.: The biggest drought events in Europe from 1950 to 2012, J. Hydrol. Regional Studies, 3, 509-524, doi:10.1016/j.ejrh.2015.01.001, 2015.

Thom, H.C.S.: A note on the Gamma distribution, Monthly Weather Rev., 86(4), 117-122, doi:10.1175/1520-0493(1958)086<0117:ANOTGD>2.0.CO;2, 1958.

Vogt, J.V., Naumann, G., Masante, D., Spinoni, J., Cammalleri, C., Erian, W., Pischke, F., Pulwarty, R. and Barbosa, P.: Drought Risk Assessment and Management: A Conceptual Framework. JRC Technical Reports, EUR 29464 EN, Publication Office of the European Union, Luxemburg, doi:10.2760/919458, 2018a.

Vogt, J.V., Barbosa, P., Cammalleri, C., Carrão, H. and Lavaysse, C.: Drought Risk Management: Needs and Experiences in Europe, in: Wilhite, D.A. and Pulwarty, R.S. (Eds.). Drought and Water Crises. Integrating Science, Management, and Policy (Chapter 18). CRC Press (Taylor &

https://doi.org/10.5194/nhess-2020-204
Preprint. Discussion started: 7 August 2020

Francis), Boca Raton, 385-407, 2018b.

Wilhite, D.A. and Pulwarty, R.S.: Drought and Water Crises: Lessons learned and the road ahead, in: Wilhite, D.A. (Eds.). Drought and Water Crises: Science, Technology, and Management Issue (Chapter 15). CRC Press (Taylor & Francis), Boca Raton, 389-398, 2005.

World Meteorological Organization (WMO): Standardized Precipitation Index User Guide (M. Svoboda, M. Hayes and D. Wood), WMO-No. 1090, Geneva, Switzerland, 16 pp, 2012.

World Meteorological Organization (WMO) and Global Water Partnership (GWP): Handbook of Drought Indicators and Indices (M. Svoboda and B.A. Fuchs). Integrated Drought Management Programme (IDMP), Integrated Drought Management Tools and Guidelines, Series 2, Geneva, Switzerland, 45 pp, 2016.

World Meteorological Organization (WMO) and Global Water Partnership (GWP): National Drought Management Policy Guidelines - A Template for Action. (D.A. Wilhite). Integrated Drought Management Programme (IDMP) Tools and Guidelines Series 1. WMO, Geneva, Switzerland and GWP, Stockholm, Sweden. ISBN: 978-92-63-11164-7 and 978-91-87823-03-9. 2014.

https://doi.org/10.5194/nhess-2020-204
Preprint. Discussion started: 7 August 2020

Table 1. Average percentage of cells in drought areas with sequencing in contrast with the "cause-effect" relationship.

Version	WARNING to WATCH	ALERT to WATCH	ALERT to WARNING
CDI-v1	4.25	1.79	1.20
CDI-v2	0.88	0.52	0.82

https://doi.org/10.5194/nhess-2020-204
Preprint. Discussion started: 7 August 2020

Natural Hazards and Earth System Sciences
Discussions

<table>
<tr><th></th><th>a</th><th>b</th><th>c</th><th>d</th><th>e</th><th>f</th><th>g</th><th>h</th></tr>
<tr><td>zSPI</td><td>= 0</td><td>= 1</td><td>= 0</td><td>= 0</td><td>= 0</td><td>= 1</td><td>= 1</td><td>= 1</td></tr>
<tr><td>zSM</td><td>≥ -1</td><td>≥ -1</td><td>< -1</td><td>≥ -1</td><td>< -1</td><td>< -1</td><td>≥ -1</td><td>< -1</td></tr>
<tr><td>zfAPAR</td><td>≥ -1</td><td>≥ -1</td><td>≥ -1</td><td>< -1</td><td>< -1</td><td>≥ -1</td><td>< -1</td><td>< -1</td></tr>
<tr><td>$zSPI_{m-1} = 0$</td><td>0</td><td rowspan="2">1</td><td colspan="3">0</td><td rowspan="2">2</td><td rowspan="2" colspan="2">3</td></tr>
<tr><td>$zSPI_{m-1} = 1$</td><td>4</td><td>4</td><td colspan="2">5</td></tr>
</table>

1 WATCH | 2 WARNING | 3 ALERT | 4 FULL RECOVERY | 5 PARTIAL RECOVERY

Figure 1. Schematic representation of the CDI-v1 computation procedure. The upper part of the table reports the eight possible combinations of the three main Boolean quantities (from *a* to *h*). The lower part of the table reports the corresponding CDI values for the two possible cases of antecedent zSPI (subscript m-1).

https://doi.org/10.5194/nhess-2020-204
Preprint. Discussion started: 7 August 2020

Natural Hazards and Earth System Sciences
Open Access
Discussions

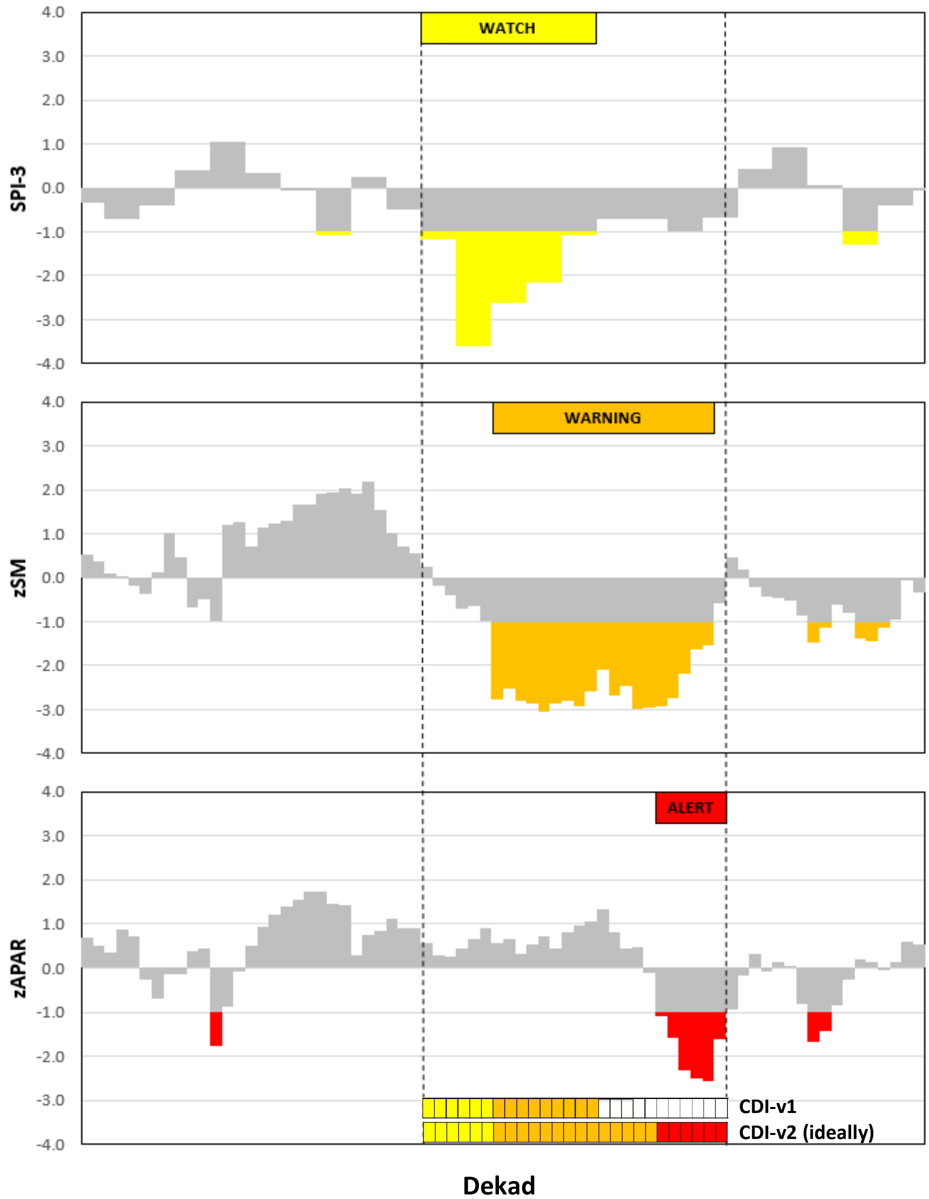

Figure 2. Example of the possible cascade process driving the evolution in a case of a drought event in Spain. Dotted lines delimit the period under drought, whereas the squares at the bottom of the plots report the outcome of the operational CDI (CDI-v1, upper line) and the ideal evolution of a revised version (CDI-v2 ideally, lower line) values for each dekad.

https://doi.org/10.5194/nhess-2020-204
Preprint. Discussion started: 7 August 2020

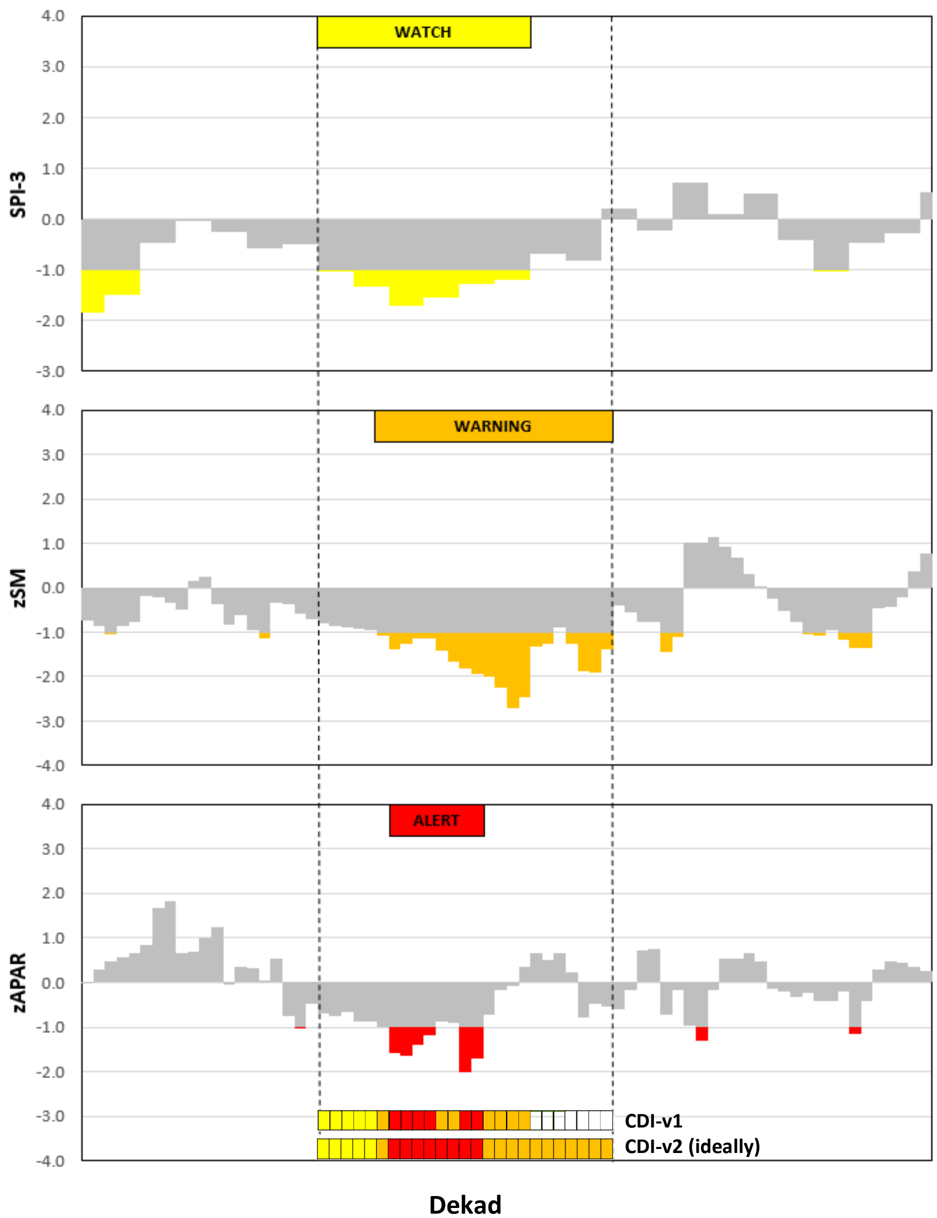

Figure 3. Example of the small gaps that can occur during a drought event in France. Dotted lines delimit the period under drought, whereas the squares at the bottom of the plots report the outcome of the operational CDI (CDI-v1, upper line) and the ideal evolution of a revised version (CDI-v2 ideally, lower line) values for each dekad.

https://doi.org/10.5194/nhess-2020-204
Preprint. Discussion started: 7 August 2020

Natural Hazards and Earth System Sciences
Open Access
EGU
Discussions

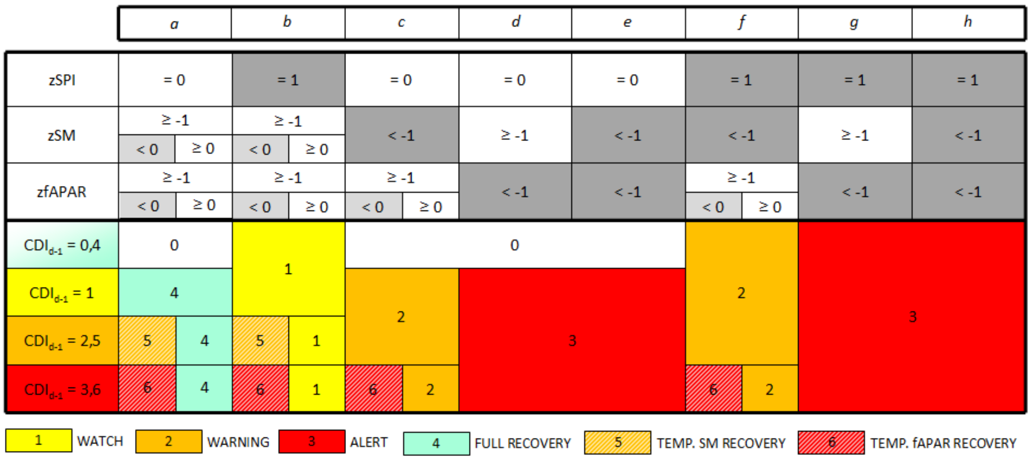

Figure 4. Schematic representation of the CDI-v2 computation procedure. The upper part of the table reports the eight possible combinations of the three main Boolean quantities (from *a* to *h*), with sub-cases (based on the second set of thresholds) reported where used. The lower part of the table reports the corresponding CDI values for all the antecedent CDI values (subscript d-1).

https://doi.org/10.5194/nhess-2020-204
Preprint. Discussion started: 7 August 2020

Natural Hazards and Earth System Sciences
Open Access
Discussions

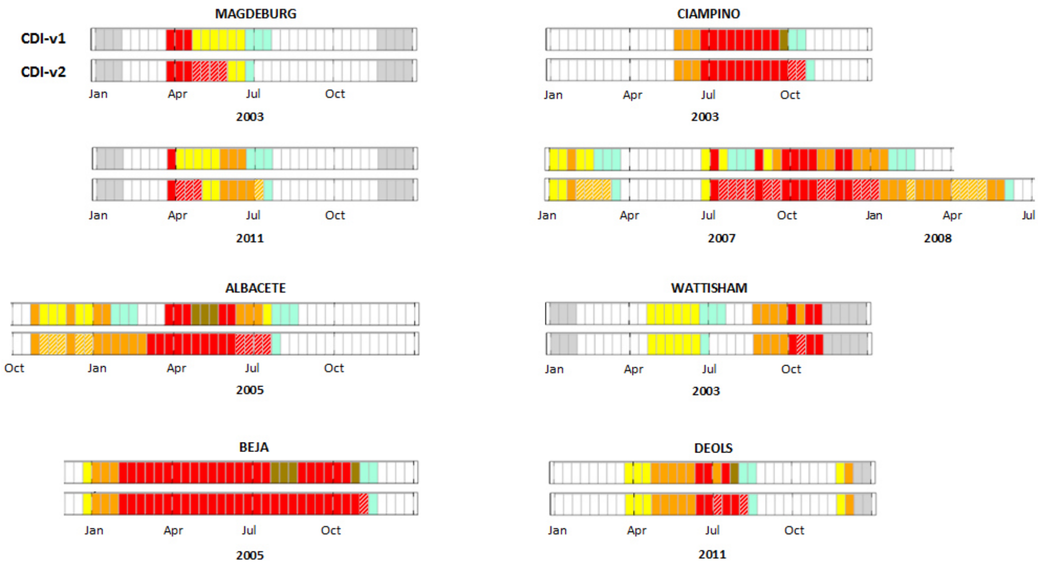

Figure 5. Timeseries of CDI-v1 (upper lines) and CDI-v2 (lower lines) for different test sites under drought between 2001 and 2011, as documented in Sepulcre-Canto et al. (2012). See Figs. 1 and 4 for the corresponding legends. The labels in the x-axis correspond to the beginning of the month.

Figure 6. Timeseries of CDI-v1 (upper lines) and CDI-v2 (lower lines) for different test sites under drought between 2012 and 2018, as documented in the analytical drought reports in EDO (https://edo.jrc.ec.europa.eu/edov2/php/index.php?id=1051). See Figs. 1 and 4 for the corresponding legends. The labels in the x-axis correspond to the beginning of the month.

https://doi.org/10.5194/nhess-2020-204
Preprint. Discussion started: 7 August 2020

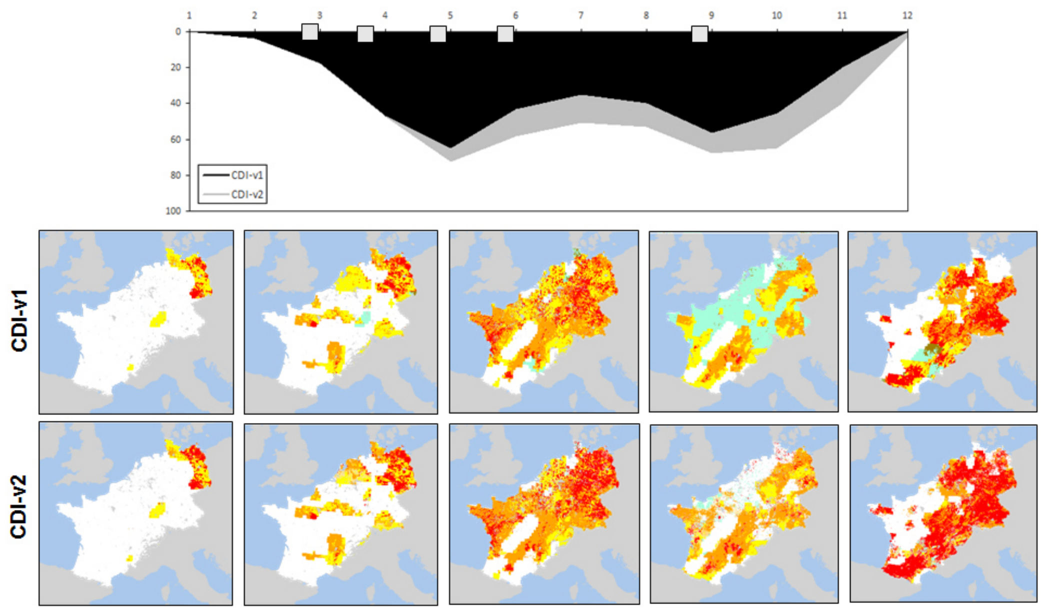

Figure 7. Temporal evolution of the 2003 central Europe drought according to the two versions of the CDI. The upper plot shows the percentage of the area under drought (in black for CDI-v1 and in grey for CDI-v2), whereas the lower images depict the spatial distribution of the CDI-v1 (upper row) and CDI-v2 (lower row) for the selected dekads (demarked in the upper plot by the squares on the x-axis).

https://doi.org/10.5194/nhess-2020-204
Preprint. Discussion started: 7 August 2020

545 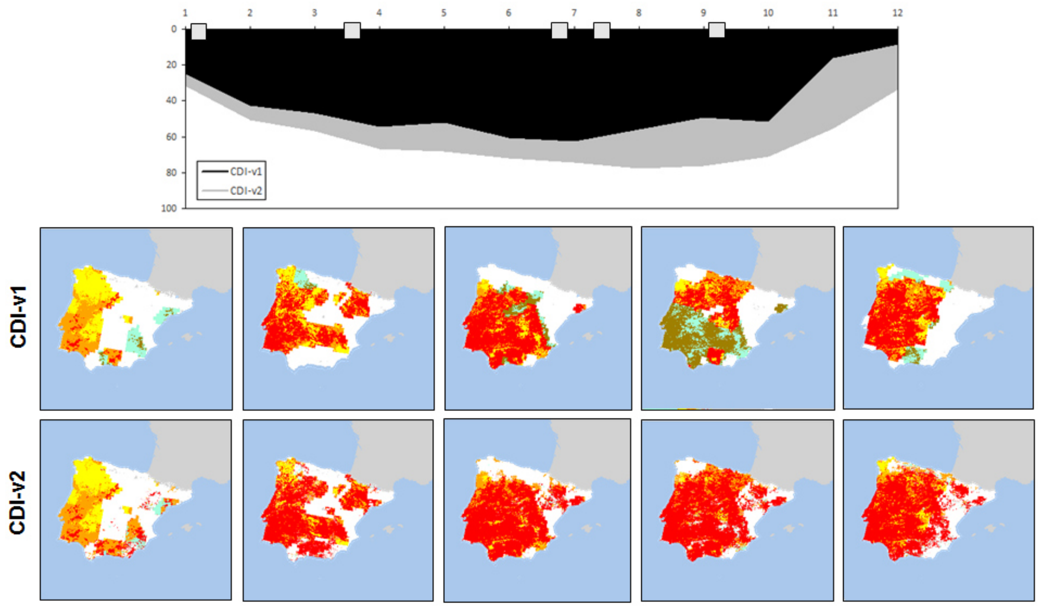

546 **Figure 8.** Temporal evolution of the 2005 Iberian Peninsula drought according to the two versions of the CDI. The upper plot shows the percentage of the area under drought (in black for CDI-v1 and in grey for CDI-v2), whereas the lower images depict the spatial distribution of the CDI-v1 (upper row) and CDI-v2 (lower row) for the selected dekads (demarked in the upper plot by the squares on the x-axis).

https://doi.org/10.5194/nhess-2020-204
Preprint. Discussion started: 7 August 2020

Natural Hazards and Earth System Sciences
Open Access
Discussions

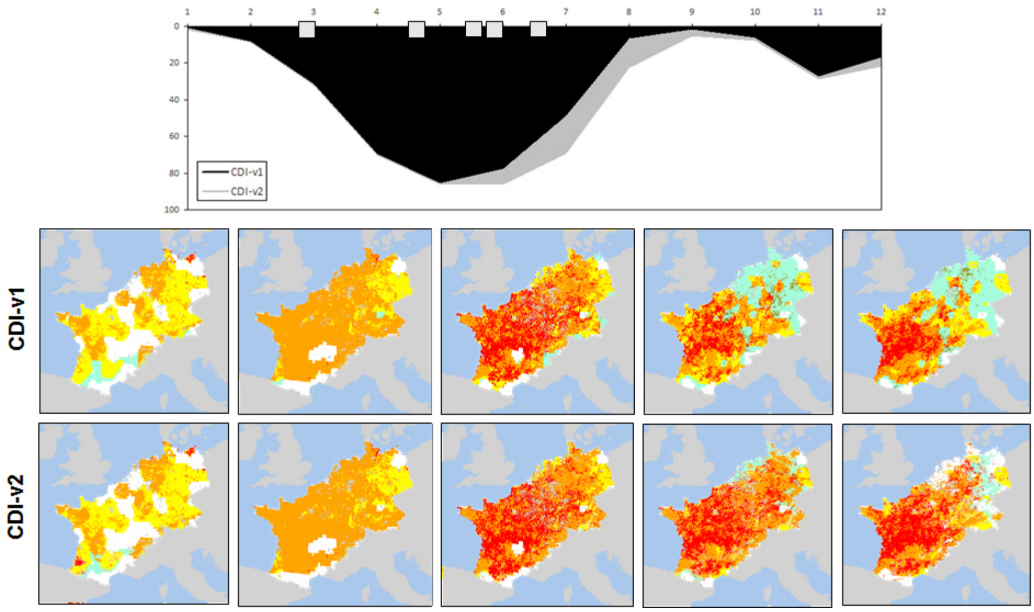

Figure 9. Temporal evolution of the 2011 central Europe drought according to the two versions of the CDI. The upper plot shows the percentage of the area under drought (in black for CDI-v1 and in grey for CDI-v2), whereas the lower images depict the spatial distribution of the CDI-v1 (upper row) and CDI-v2 (lower row) for few selected dekads (demarked in the upper plot by the squares on the x-axis).

https://doi.org/10.5194/nhess-2020-204
Preprint. Discussion started: 7 August 2020

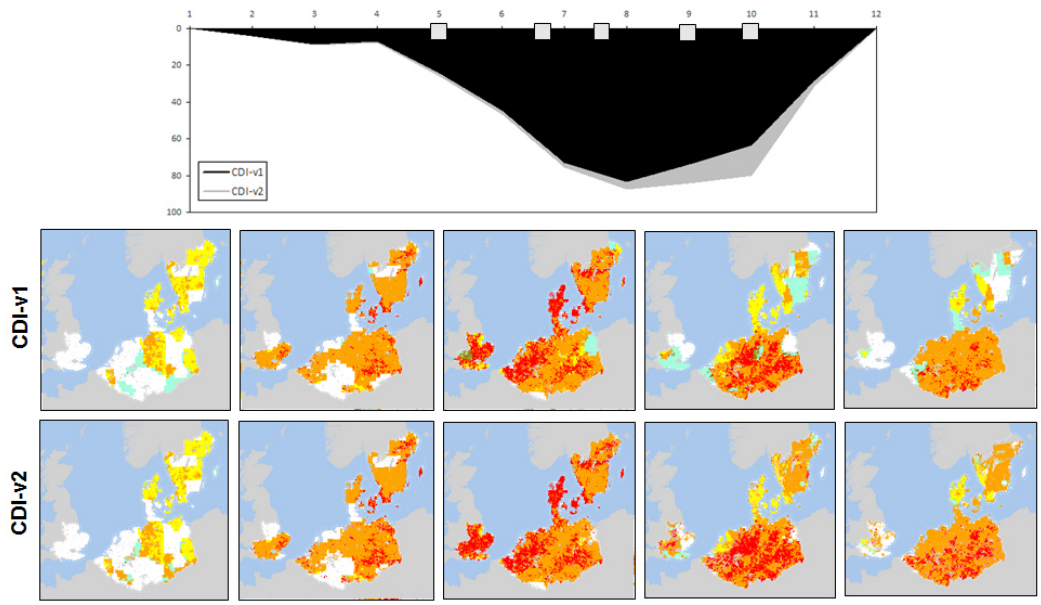

Figure 10. Temporal evolution of the 2018 northern Europe drought according to the two versions of the CDI. The upper plot shows the percentage of the area under drought (in black for CDI-v1 and in grey for CDI-v2), whereas the lower images depict the spatial distribution of the CDI-v1 (upper row) and CDI-v2 (lower row) for the selected dekads (demarked in the upper plot by the squares on the x-axis).

https://doi.org/10.5194/nhess-2020-204
Preprint. Discussion started: 7 August 2020

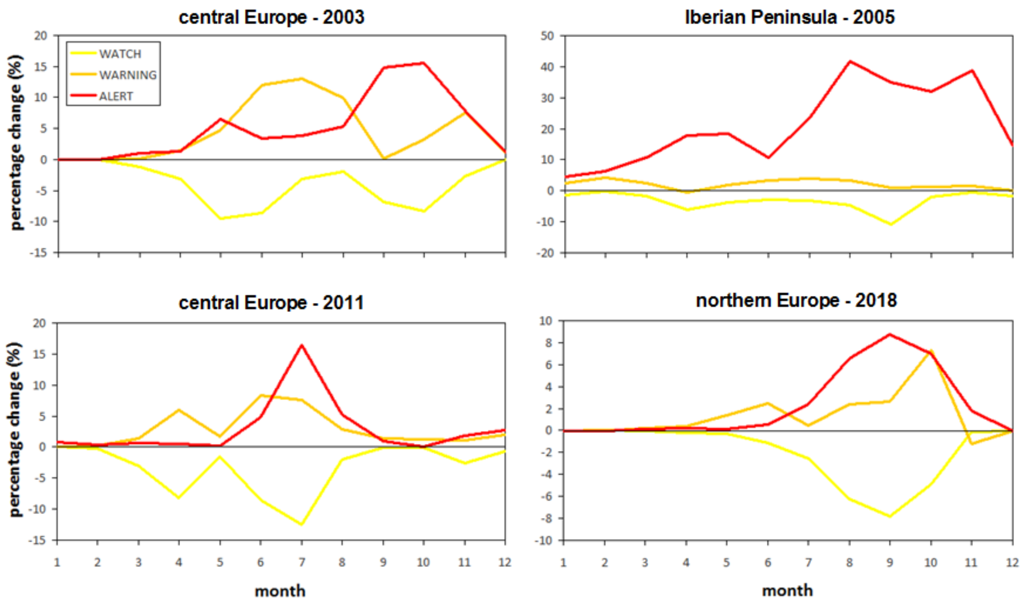

Figure 11. Percentage differences between CDI-v1 and CDI-v2 fraction of area in WATCH (yellow line), WARNING (orange line) and ALERT (red line) stages for the same four main droughts depicted in Figs. 7-10. Negative (positive) values indicate a reduction (increase) in the CDI-v2 compared to CDI-v1.